# Studies in bank voles reveal strain differences between chronic wasting disease prions from Norway and North America

Romolo Nonno[a,1], Michele A. Di Bari[a], Laura Pirisinu[a], Claudia D'Agostino[a], Ilaria Vanni[a], Barbara Chiappini[a], Stefano Marcon[a], Geraldina Riccardi[a], Linh Tran[b], Turid Vikøren[b], Jørn Våge[b], Knut Madslien[b], Gordon Mitchell[c], Glenn C. Telling[d], Sylvie L. Benestad[b,2], and Umberto Agrimi[a,2]

[a]Department of Food Safety, Nutrition and Veterinary Public Health, Istituto Superiore di Sanità, 00161 Rome, Italy; [b]World Organization for Animal Health Reference Laboratory for Chronic Wasting Disease, Norwegian Veterinary Institute, N-0106 Oslo, Norway; [c]National and World Organization for Animal Health Reference Laboratory for Scrapie and Chronic Wasting Disease, Canadian Food Inspection Agency, Ottawa, ON K2H 8P9, Canada; and [d]Prion Research Center, Department of Microbiology, Immunology and Pathology, Colorado State University, Fort Collins, CO 80525

Chronic wasting disease (CWD) is a relentless epidemic disorder caused by infectious prions that threatens the survival of cervid populations and raises increasing public health concerns in North America. In Europe, CWD was detected for the first time in wild Norwegian reindeer (*Rangifer tarandus*) and moose (*Alces alces*) in 2016. In this study, we aimed at comparing the strain properties of CWD prions derived from different cervid species in Norway and North America. Using a classical strain typing approach involving transmission and adaptation to bank voles (*Myodes glareolus*), we found that prions causing CWD in Norway induced incubation times, neuropathology, regional deposition of misfolded prion protein aggregates in the brain, and size of their protease-resistant core, different from those that characterize North American CWD. These findings show that CWD prion strains affecting Norwegian cervids are distinct from those found in North America, implying that the highly contagious North American CWD prions are not the proximate cause of the newly discovered Norwegian CWD cases. In addition, Norwegian CWD isolates showed an unexpected strain variability, with reindeer and moose being caused by different CWD strains. Our findings shed light on the origin of emergent European CWD, have significant implications for understanding the nature and the ecology of CWD in Europe, and highlight the need to assess the zoonotic potential of the new CWD strains detected in Europe.

prions | prion strains | TSE | chronic wasting disease | CWD

**P**rion diseases, otherwise known as transmissible spongiform encephalopathies (TSEs), are invariably fatal infectious neurodegenerative disorders of animals and humans. Prions are composed largely or exclusively of self-replicating protein aggregates of PrP$^{Sc}$, which is a misfolded isoform of the cellular prion protein (PrP$^C$). Most human prion diseases, including Creutzfeldt–Jakob disease (CJD) and sporadic fatal insomnia, occur sporadically and are thought to result from the spontaneous misfolding of PrP$^C$ into PrP$^{Sc}$. Mutations in the coding sequence of the gene encoding PrP (*PRNP*) in inherited diseases such as familial CJD, fatal familial insomnia, and Gerstmann–Sträussler–Scheinker syndrome are thought to potentiate spontaneous misfolding of PrP$^C$ to PrP$^{Sc}$ (1). The intrinsic transmissibility of prions has also resulted in epidemics of acquired prion diseases (2), with significant public health consequences. Examples include iatrogenic CJD transmission caused by prion-contaminated human growth hormone preparations and dura mater grafts, and variant CJD resulting from human exposure to bovine spongiform encephalopathy (BSE) prions.

Animal prion diseases also occur as contagious forms giving rise to outbreaks such as classical scrapie in small ruminants and chronic wasting disease (CWD) in cervids (3). In addition to their impact on human health, exemplified by zoonotic BSE

transmission (2), epidemic animal prion diseases, such as CWD in North America (NA) (4), have significant ecologic and economic consequences. First identified in captive deer in Northern Colorado in the 1960s, CWD is now known to affect wild and farmed cervid populations in 26 states and three Canadian provinces. Disease was introduced to the Republic of Korea following importation of subclinical elk (*Cervus canadensis*) from Canada (5). The irrevocable spread of CWD in NA raises serious concerns about the survival of cervid populations, as well as for the risks posed to other animals and to humans (6).

Prion diseases are caused by different prion strains, which are thought to be encoded by conformational variants of PrP$^{Sc}$ (7, 8). While different PrP$^{Sc}$ conformers can be discriminated using biochemical approaches, assessing infectious properties of prions in susceptible hosts remains the gold standard for strain characterization. Such analyses are of the utmost importance for trace-back studies of iatrogenic (9, 10) or zoonotic prion strains (11, 12), for identifying spillover hosts (13), for estimating the zoonotic potential of classical and atypical scrapie strains (14,

**Significance**

Chronic wasting disease (CWD) is a highly contagious disease caused by prions that affects several cervid species and is relentlessly spreading across North America. Very recently, CWD was detected for the first time in Europe. In this study, we found that Norwegian CWD strains are distinct from those causing the epidemic in North America. Moreover, we show that Norwegian reindeer and moose are affected by different CWD strains, revealing an unprecedented prion strain variation in Norwegian wild cervid populations. These findings indicate that North American CWD prions are not the proximate cause of the newly discovered Norwegian CWD cases and have implications for CWD control strategies in Europe, as well as for the safety of humans.

15), and for understanding the epidemiology and evolution of strains in contagious prion diseases (16–20).

In Europe, CWD was detected for the first time in wild Norwegian reindeer (*Rangifer tarandus*) and moose (*Alces alces*) in 2016 (21, 22). The emergence of CWD in Europe necessitates characterization of the strain properties of these CWD prions of uncertain origin to explore a possible link with NA CWD. Knowledge about Norwegian CWD strains is essential to assess their risk to animal and human health, and to develop evidence-based policies to control and limit the spread of the disease (23).

In a previous study, we found that bank voles carrying isoleucine at codon 109 (Bv109I) are highly susceptible to CWD isolates from the United States. After subpassage in Bv109I, the same vole-adapted CWD strain was isolated from NA mule deer (*Odocoileus hemionus*), white-tailed deer (*Odocoileus virginianus*), and elk isolates, which was characterized by an unprecedented short disease duration and peculiar and recognizable strain features (24). Here, we extended our previous characterizations of NA CWD isolates and compared the biological properties of CWD isolates from Norway and NA by transmission to the Bv109I genetic line of bank voles.

## Results

### Bank Voles Are Susceptible to Canadian and Norwegian CWD Isolates.
We selected Norwegian and Canadian CWD isolates (Table 1) whose molecular and pathological features have been previously reported (22). Direct comparison of the PrP$^{Sc}$ types in the brain homogenates used for the present bioassay studies (*SI Appendix*, Fig. S1) confirmed that the three Norwegian moose CWD cases are characterized by PrP$^{Sc}$ features different from the Canadian isolates, while Norwegian reindeer share PrP$^{Sc}$ characteristics with NA isolates (22).

All Bv109I inoculated with Canadian CWD isolates from elk (E-CA1 and E-CA2) and white-tailed deer (D-CA1) developed clinical disease with short incubation times (Table 1). In contrast, the Canadian moose inoculum (M-CA1) produced an incomplete attack rate and a longer mean survival time, largely explained by the extremely long survival time of a single Bv109I (*SI Appendix*, Fig. S2). The less efficient transmission of this Canadian moose isolate is consistent with a low prion infectious titer; this interpretation is supported by the lower level of PrP$^{Sc}$ in this inoculum compared to other Canadian isolates (*SI Appendix*, Fig. S1).

Bv109I inoculated with Norwegian moose isolates M-NO1, M-NO2, and M-NO3 developed CWD with longer disease kinetics compared to Canadian CWD isolates (Table 1). Transmission of Norwegian reindeer CWD isolates (R-NO1 and R-NO2) was inefficient, with only one R-NO1 inoculated vole developing disease, and no voles succumbing to disease after challenge with R-NO2. These negative and inefficient transmissions are not the result of low levels of PrP$^{Sc}$ in brain homogenates of these Norwegian CWD isolates (*SI Appendix*, Fig. S1).

Overall, three different patterns of transmission in Bv109I were observed from 1) Canadian isolates (short survival time), 2) Norwegian moose (long survival time), and 3) Norwegian reindeer (barely transmissible in Bv109I) (*SI Appendix*, Fig. S2).

### Different PrP$^{Sc}$ Types in Bv109I Infected with Different CWD Sources.
All Bv109I that developed CWD upon primary transmission accumulated proteinase K (PK)-resistant PrP$^{Sc}$ (PrP$^{res}$) in their brains, which was characterized by Western blotting (WB) with monoclonal antibodies (mAbs) directed to different PrP epitopes.

Bv109I infected with Canadian CWD isolates showed low levels of PrP$^{res}$, having uniform glycosylation pattern and ~17- to 18-kDa apparent molecular weight (MW) (Fig. 1*A*) (MW values refer to the unglycosylated PrP$^{res}$ fragments). This electrophoretic pattern was similar to that previously observed in Bv109I infected with US CWD isolates (Fig. 1*A*).

In contrast, Bv109I infected with Norwegian moose isolates were all characterized by the presence of an additional faster migrating C-terminal PrP$^{res}$ of ~12- to 13-kDa MW, accompanied by glycosylated fragments that overlapped with the main PrP$^{res}$ signal (Fig. 1*A*). This characteristic was also a feature of PrP$^{res}$ in the Norwegian moose brain samples (22) (*SI Appendix*, Fig. S1) and was thus preserved after transmission in voles. Interestingly, when focusing on the main PrP$^{res}$ fragment in voles infected with the Norwegian moose isolates, we found that the MW of PrP$^{res}$ varied according to the inoculum, with voles infected with M-NO1 showing a higher MW than those infected with M-NO2 and M-NO3 (Fig. 1*A*, mAb Sha31). Epitope mapping confirmed that these different apparent MWs depended on different PK cleavage sites on PrP$^{Sc}$ (*SI Appendix*, Fig. S3).

The single Bv109I infected with R-NO1 showed a PrP$^{Sc}$ type different from Bv109I infected with Norwegian moose, because of the absence of the 12- to 13-kDa additional PrP$^{res}$ fragment, and with MW of PrP$^{res}$ higher than Bv109I infected with Canadian isolates or with M-NO2 and M-NO3 (Fig. 1*A* and *SI Appendix*, Fig. S3).

**Table 1. Transmission and adaptation in Bv109I of Canadian and Norwegian CWD isolates from different cervid species**

| | | | Transmission in Bv109I | | | | | |
|---|---|---|---|---|---|---|---|---|
| Inocula | | | Primary transmission | | Second passage | | Third passage | |
| Origin | Species | ID in the paper | Survival time* | Attack rate‡ | Survival time* | Attack rate‡ | Survival time* | Attack rate‡ |
| Canada | Elk | E-CA1 | 225 ± 71 | 13/13 | 58 ± 8 | 10/10 | 35 ± 3 | 13/13 |
| Canada | Elk | E-CA2 | 210 ± 69 | 14/14 | 37 ± 3 | 9/9 | ND | ND |
| Canada | WTD | D-CA1 | 147 ± 14 | 13/13 | 53 ± 13 | 11/11 | ND | ND |
| Canada | Moose | M-CA1 | 311 ± 200 | 5/10 | 41 ± 5 | 10/10 | 32 ± 3 | 12/12 |
| Norway | Moose | M-NO1 | 318 ± 41 | 10/12 | 78 ± 4 | 10/10 | 76 ± 3 | 7/7 |
| Norway | Moose | M-NO2 | 459 ± 55 | 15/15 | 211 ± 18 | 8/8 | 175 ± 36 | 7/7 |
| Norway | Moose | M-NO3 | 312 ± 46 | 13/13 | >190§ | 0/12 | ND | ND |
| Norway | Reindeer | R-NO1 | 776 | 1/7 | 113 ± 4 | 12/12 | 105 ± 9 | 11/11 |
| Norway | Reindeer | R-NO2 | >690¶ | 0/14 | ND | ND | ND | ND |

*Expressed as days postinoculation ± SD.
‡Number of positive voles/number of inoculated voles.
§Ongoing experiment; inoculated Bv109I are healthy at the indicated days postinoculation.
¶Ongoing experiment; one inoculated Bv109I is healthy at the indicated days postinoculation, and all other Bv109I were negative at postmortem.
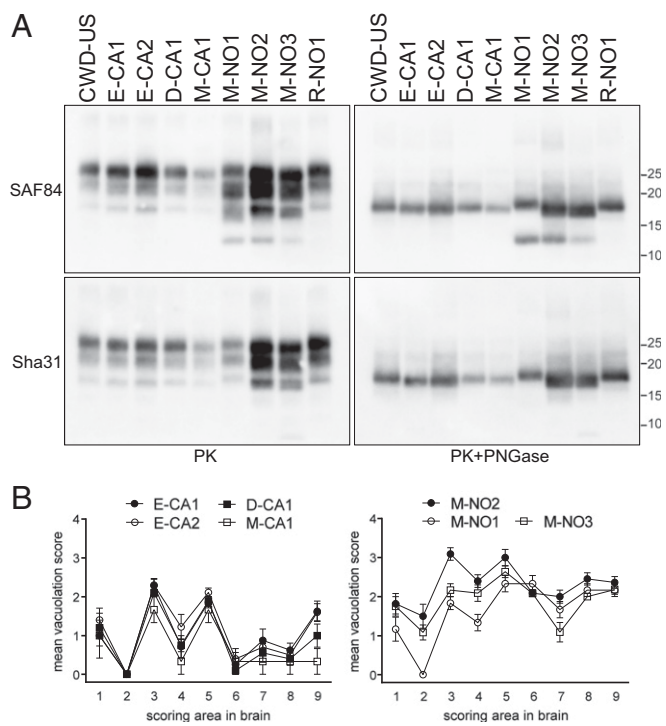
**Fig. 1.** PrP^Sc types and neurodegeneration in Bv109I infected with CWD isolates. (*A*) Representative replica Western blots showing PK-treated (PK) or PK-treated and deglycosylated (PK+PNGase) PrP^Sc from the brains of voles inoculated with the CWD isolates indicated on the *Top* of the blots, and analyzed with mAbs recognizing different epitopes on PrP, as indicated on the *Left* of the blots (SAF84 epitope at 167 to 173; Sha31 epitope at 146 to 153). The CWD inocula are indicated as in Table 1; CWD-US in the first lane indicates a Bv109I inoculated in a previous study (24) with an elk CWD isolate from the United States, here analyzed for comparison purposes. The positions of MW markers are indicated on the *Right* of the blots (in kilodaltons). Note that a PrP^res fragment migrating at ~12 to 13 kDa was detected by SAF84 only in Bv109I inoculated with Norwegian moose isolates. This PrP^res fragment was C-terminal and N-glycosylated, as it was not recognized by the more N-terminal Sha31 mAb and was enriched upon removal of N-linked sugars. (*B*) Lesion profiles in groups of Bv109I infected with CWD isolates from Canadian cervids (*Left*) or Norwegian moose (*Right*). Data points represent the mean ± SEM of at least five voles per group. Brain-scoring areas: medulla (1), cerebellum (2), superior colliculus (3), hypothalamus (4), thalamus (5), hippocampus (6), septum (7), retrosplenial and adjacent motor cortex (8), and cingulate and adjacent motor cortex (9).

### Different Neuropathological Phenotypes in Bv109I Infected with Different CWD Sources.

The brain of all CWD-affected Bv109I showed spongiform degeneration, neuronal loss, and gliosis. Semiquantitative assessment by brain lesion profiling (25, 26) showed that the extent and regional distribution of spongiform degeneration varied depending on the source of inoculum. The four Canadian CWD isolates induced very similar neuropathological profiles in voles, reminiscent of those induced by US CWD isolates (24), with the main involvement of the superior colliculus, the thalamus, and to a lesser extent, the cerebral cortex (Fig. 1*B*). In contrast, spongiosis was widespread in Bv109I infected with the Norwegian moose inocula, involving brain areas that were largely spared in Bv109I infected with Canadian CWD isolates, such as the hypothalamus and the hippocampus (Fig. 1*B*). The single diseased Bv109I following inoculation with Norwegian reindeer CWD showed spongiosis in the geniculate nuclei and the thalamus, and few scattered perivascular plaques in the meningeal space between the geniculate nuclei and the hippocampus (*SI Appendix*, Fig. S4). These features were not detected in Bv109I inoculated with any of the other CWD isolates.

PrP^Sc deposition was mainly detected in brain areas showing spongiform degeneration. In Bv109I infected with Canadian CWD isolates, PrP^Sc deposition was generally mild and restricted to specific brain areas, such as the thalamus, substantia nigra, geniculate, and vestibular nuclei. In contrast, PrP^Sc deposition was strong and widely distributed in Bv109I infected with Norwegian moose isolates (Fig. 2). Furthermore, PrP^Sc was mostly detected as diffuse, finely punctuate deposits in the neuropil of Bv109I infected with Canadian isolates, while it was mainly intraneuronal in Bv109I infected with Norwegian moose isolates (Fig. 2), thus reflecting the intraneuronal PrP^Sc deposition pattern that mainly characterizes CWD-affected moose in Norway (22). This feature was less evident in some brain areas of Bv109I infected with M-NO3, such as the cortex and hippocampus, where scattered coarse aggregates or microplaques were also observed (Fig. 2). Finally, the single Bv109I infected with R-NO1 showed a PrP^Sc deposition pattern similar to Bv109I infected with Canadian CWD isolates, but with an additional strong and diffuse PrP^Sc accumulation in some areas of the visual cortex (Fig. 2). The plaques observed in hematoxylin- and eosin-stained
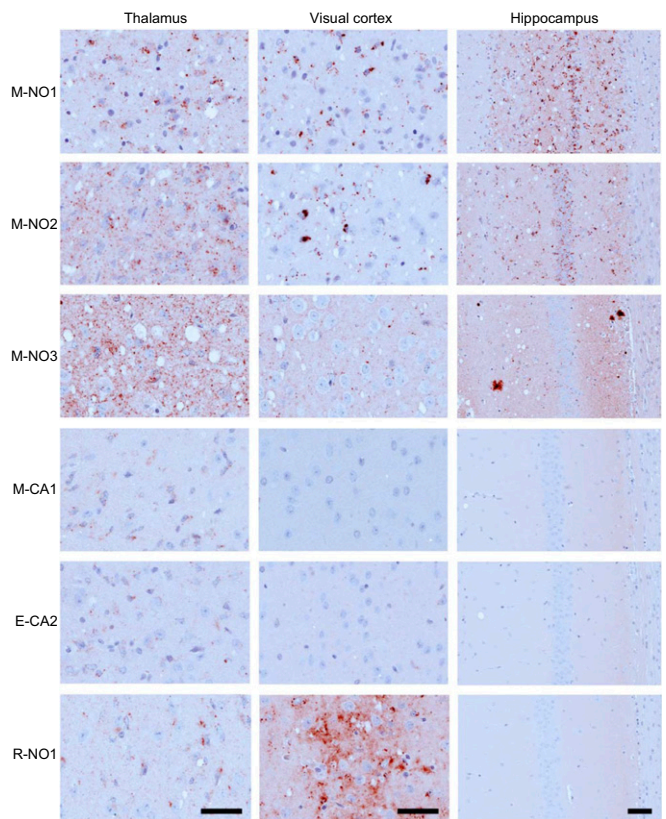


**Fig. 2.** Immunohistochemical patterns of PrP^Sc deposition in Bv109I inoculated with CWD isolates. Immunohistochemical detection of PrP^Sc in the thalamus, visual cortex (third layer), and hippocampus of Bv109I inoculated with the CWD isolates indicated on the *Left*. Norwegian moose isolates (M-NO1, M-NO2, and M-NO3) were characterized by strong PrP^Sc deposition in all brain areas, which was mainly intraneuronal, particularly in the case of M-NO1 and M-NO2. In contrast, PrP^Sc deposition was milder in Bv109I inoculated with Canadian isolates M-CA1 and E-CA2 and was mainly detected as diffuse deposits in the thalamus. The only Bv109I that was positive after inoculation of R-NO1 was characterized by a strong and diffuse PrP^Sc deposition in the visual cortex. PrP^Sc was detected by mAb SAF84. (Scale bar: 50 μm.)

sections from this vole were strongly labeled by anti-PrP antibodies (*SI Appendix*, Fig. S4).

The results of primary transmissions thus revealed three different neuropathological and PrP<sup>Sc</sup> phenotypes in Bv109I inoculated with CWD from Canadian cervids, Norwegian moose, and Norwegian reindeer. These differences reflected the three different transmission patterns displayed by CWD isolates (i.e., short survival time, long survival time, and low/no transmission, respectively). The pathological features induced by the Canadian isolates were strongly reminiscent of those induced by CWD isolates from the United States (24).

**Different Vole-Adapted Strains Were Isolated from Canadian and Norwegian CWD Isolates.** In our previous experiments with US CWD isolates, the survival time upon second passage in Bv109I ranged from 34 to 44 d postinoculation (dpi) and invariably shortened to ~35 dpi on further subpassage. This rapid time to disease onset is remarkable for a prion disease and can be considered a pathognomonic marker of this Bv109I-adapted CWD strain (24). In order to investigate whether the same Bv109I-adapted strain previously detected in US isolates could be isolated from CWD isolates from Canada and Norway, we inoculated groups of Bv109I with brain homogenates from Bv109I affected after primary transmission with the different CWD isolates.

Second passages resulted in adaptation of the CWD agents, characterized by a shortening of survival times (Table 1). Canadian CWD isolates resulted in extremely short survival times (between 37 and 58 dpi), equivalent to those previously observed with US isolates. None of the second passages in Bv109I infected with Norwegian CWD isolates resulted in survival time as short as those produced by Canadian isolates (Table 1). M-NO1 and M-NO2 gave very different mean survival times of 78 and 211 dpi, respectively. A clear-cut adaptation to Bv109I occurred also for R-NO1, with survival time shortening from 776 dpi of the donor Bv109I to 113 dpi. The second passage of M-NO3 is still ongoing at the time of writing, with no evidence of clinical disease after 190 dpi.

WB analysis showed that the PrP<sup>Sc</sup> profiles observed on primary passage were mainly preserved on second passage in Bv109I. PrP<sup>Sc</sup> accumulating in the brain of Bv109I-adapted Norwegian moose isolates could be unambiguously distinguished from all other Bv109I-adapted CWD isolates by the presence of the additional mAb SAF84 reactive C-terminal PrP<sup>res</sup> of 12 to 13 kDa (Fig. 3A). The WB PrP<sup>res</sup> profile of M-NO2 slightly changed on second passage, showing lower levels of the main PrP<sup>res</sup> fragment and an increase of the 12- to 13-kDa PrP<sup>res</sup> (*SI Appendix*, Fig. S5; also compare Figs. 1A and 3A), so that 12- to 13-kDa PrP<sup>res</sup> was more prevalent in Bv109I infected with M-NO2 than in those infected with M-NO1. Bv109I-adapted M-NO1 and R-NO1 CWD isolates were characterized by a higher MW of the main PrP<sup>res</sup> (18 kDa) than all other groups (~17 to 18 kDa) (Fig. 3A, Sha31). The presence or absence of the additional 12- to 13-kDa C-terminal PrP<sup>res</sup> and the MW of the main PrP<sup>res</sup> permitted grouping the Bv109I-adapted CWD into four different PrP<sup>Sc</sup> types. One type, characterized by a single PrP<sup>res</sup> of 17 to 18 kDa, was associated with all Canadian CWD isolates. In sharp contrast, three different PrP<sup>Sc</sup> types were associated with the three Norwegian isolates: 1) 18 kDa PrP<sup>res</sup> (R-NO1), 2) 18 kDa PrP<sup>res</sup> and low amount of 12- to 13-kDa PrP<sup>res</sup> (M-NO1), and 3) 17- to 18-kDa PrP<sup>res</sup> and high amount of 12- to 13-kDa PrP<sup>res</sup> (M-NO2) (Fig. 3A).

The two distinct neuropathological patterns detected after primary transmission were also observed after subpassage (compare Figs. 1B and 3B). M-NO1 and M-NO2 showed similar lesion profiles, but there were also notable differences in some brain areas not sampled for lesion profiles, including the stronger
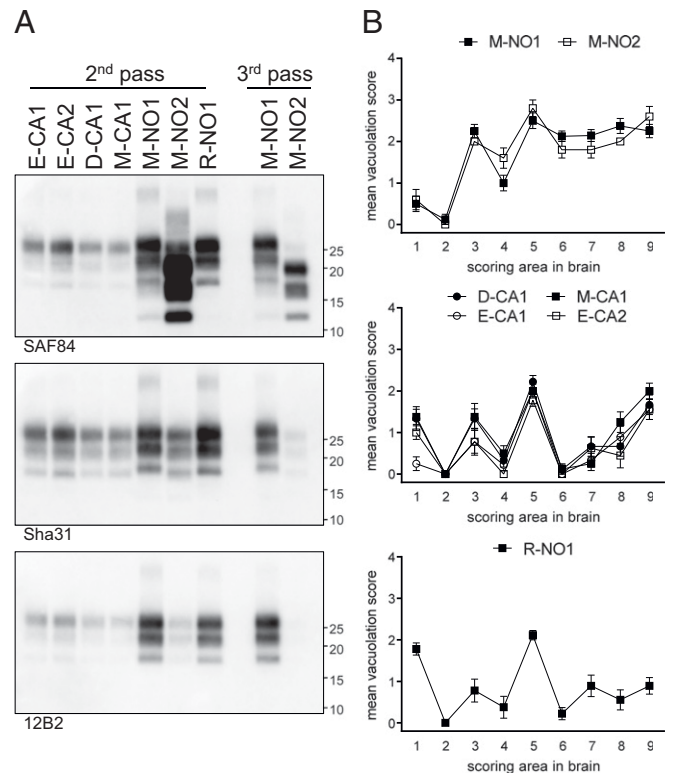


**Fig. 3.** PrP<sup>Sc</sup> types and neurodegeneration in Bv109I-adapted CWD isolates. (*A*) Representative replica Western blots showing PK-treated PrP<sup>Sc</sup> from Bv109I after second or third subpassages with the CWD isolates indicated on the *Top* of the blots, and analyzed with mAbs recognizing different epitopes on PrP, as indicated below the blots (SAF84 epitope at 167 to 173; Sha31 epitope at 146 to 153; 12B2 epitope at 93 to 97). The positions of molecular weight markers are indicated on the *Right* of the blots (in kilodaltons). Note that the PrP<sup>res</sup> fragment migrating at ~12 to 13 kDa was detected by SAF84 only in Bv109I after second and third passages with Norwegian moose isolates and was much more abundant in M-NO2 than in M-NO1. Furthermore, in M-NO2 there was a decrease of the main PrP<sup>res</sup> fragment at the third passage (Sha31 blot), which was also reflected in a decreased 12B2 binding. The blot detected with Sha31 shows that PrP<sup>res</sup> in M-NO1 (second and third passages) and R-NO1 migrates slightly higher than in E-CA1, E-CA2, D-CA1, M-CA1, and M-NO2 (second and third passages). This was reflected in a better preservation of the N-terminal 12B2 epitope as evidenced by the partial loss of PrP<sup>res</sup> signal in E-CA1, E-CA2, D-CA1, M-CA1, and M-NO2, but not in M-NO1 and R-NO1, in the blot detected with 12B2. (*B*) Lesion profiles in groups of Bv109I after two passages with CWD isolates from Norwegian moose (*Upper*), Canadian cervids (*Middle*), or Norwegian reindeer (*Lower*). Data points represent the mean (SEM) of at least five voles per group. Brain-scoring areas: medulla (1), cerebellum (2), superior colliculus (3), hypothalamus (4), thalamus (5), hippocampus (6), septum (7), retrosplenial and adjacent motor cortex (8), and cingulate and adjacent motor cortex (9).

involvement of some white matter tracts in Bv109I infected with M-NO2 (*SI Appendix*, Fig. S6). The four Bv109I-adapted Canadian CWD isolates showed overlapping lesion profiles, which were also partially similar to Bv109I-adapted R-NO1 (Fig. 3B).

These two different neuropathological patterns were paralleled by different patterns of PrP<sup>Sc</sup> distribution in the same brain areas, as detected by paraffin-embedded tissue (PET) blot (Fig. 4). The specific neurotropism of the CWD agents is further exemplified by the different layering of PrP<sup>Sc</sup> deposition in cerebral cortices, where PrP<sup>Sc</sup> accumulated in all layers in Bv109I-adapted M-NO1 and M-NO2, while it only deposited in the deepest layers in the Bv109I-adapted Canadian CWD isolates.

The overall neuropathological phenotype of the Norwegian R-NO1 in Bv109I was similar to CWD isolates from Canada,
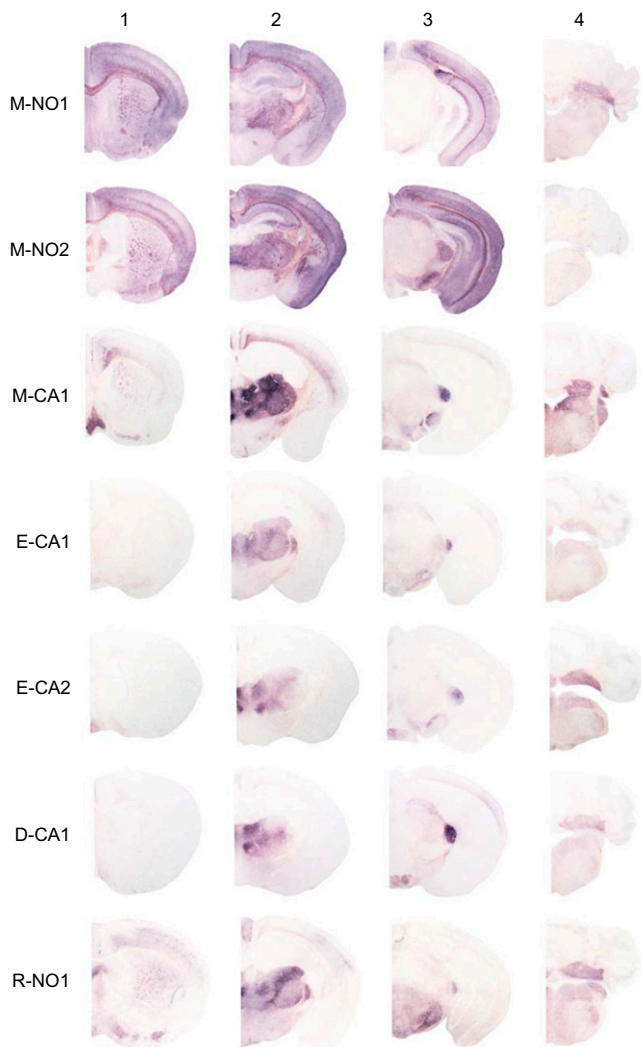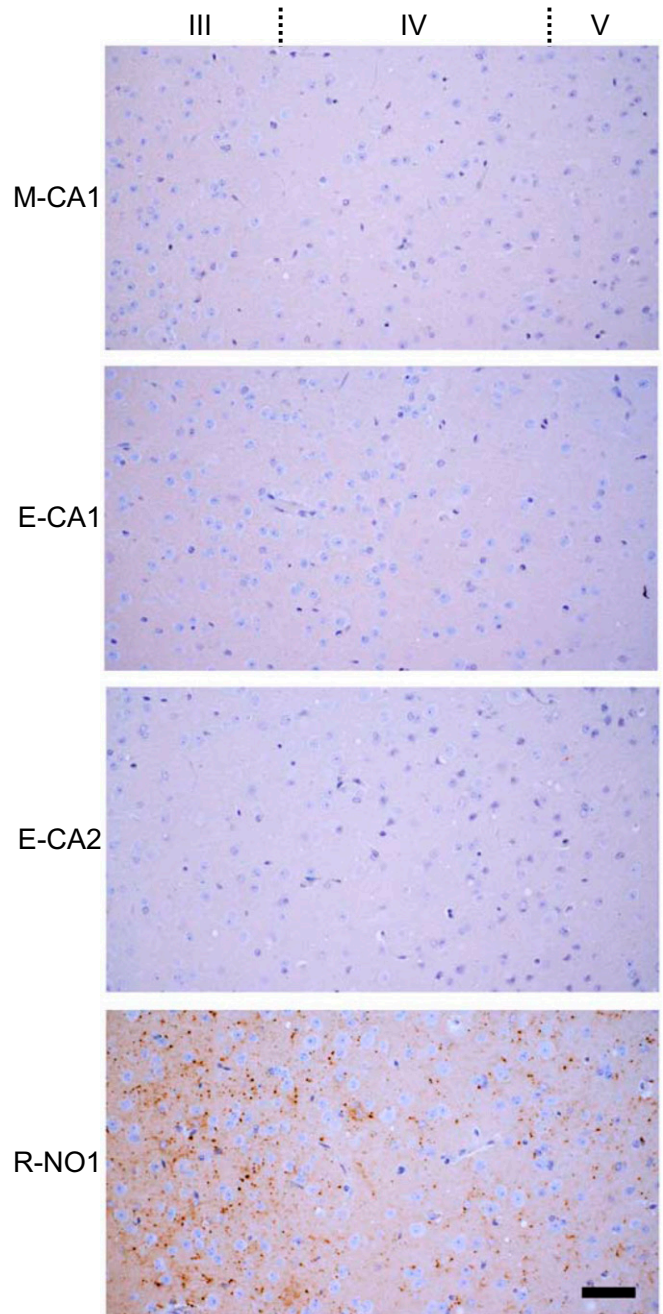
**Fig. 4.** Different patterns of PrP$^{Sc}$ deposition in Bv109I-adapted CWD isolates. PET blot detection of protease-resistant PrP$^{Sc}$ in coronal sections of the forebrain, representing telencephalon (1), diencephalon (2), midbrain (3), and hindbrain (4) from representative Bv109I following two passages with the CWD isolates indicated on the *Left*. PrP$^{Sc}$ was detected with mAb SAF84.

paralleling the findings in the original host (21). Nevertheless, Bv109I-adapted R-NO1 showed a more widespread involvement of some cortical areas (Fig. 4), where diffuse and punctate PrP$^{Sc}$ deposition was observed in all cortical layers (Fig. 5). In addition, different WB patterns and incubation times were observed in the Bv109I-adapted R-NO1 compared to the Bv109I-adapted Canadian isolates. Thus, after two passages in Bv109I, analyses of neuropathological changes, PrP$^{Sc}$ profiles, and incubation times suggest the isolation of four different strains: one derived from the Canadian isolates and three from Norwegian isolates.

**Further Characterization of Three Novel Norwegian CWD Strains during Third Passage in Bank Voles.** We previously found that certain second passages from individual Bv109I infected with US CWD isolates resulted in longer than expected survival times and required further subpassaging for full adaptation (24). In order to investigate whether further adaptation in Bv109I could lead to convergence of Bv109I-adapted CWD isolates, we conducted additional subpassages of Bv109I-adapted Norwegian isolates and two Bv109I-adapted Canadian isolates.

Third passage of Canadian isolates (E-CA1 and M-CA1) confirmed the isolation of the same CWD strain previously isolated from US CWD isolates, characterized by the extremely short survival time of 35 dpi (Table 1). Conversely, none of the Bv109I-adapted Norwegian isolates showed substantial shortening of the disease course, which was much slower than with Bv109I-adapted Canadian isolates and resulted in three different survival times of 76 dpi (M-NO1), 175 dpi (M-NO2), and 105 dpi (R-NO1) (Table 1).



**Fig. 5.** Different patterns of PrP$^{Sc}$ deposition in cortical layers of Bv109I-adapted CWD isolates. Immunohistochemical detection of PrP$^{Sc}$ in the third, fourth, and fifth cortical layers of the somatosensory cortex of Bv109I after second passage with the CWD isolates indicated on the *Left*. PrP$^{Sc}$ was not detected in Bv109I infected with the Canadian CWD isolates but was found as diffuse and punctate deposits in all layers of Bv109I infected with R-NO1. PrP$^{Sc}$ was detected by mAb SAF84. (Scale bar: 50 μm.)

The characterization of disease phenotypes further confirmed the isolation of two new distinct CWD strains from M-NO1 and M-NO2. Interestingly, we noticed that M-NO1 and M-NO2 followed different patterns of adaptation in Bv109I. While the phenotypes of disease were stable in M-NO1, they were slightly modified in M-NO2 during Bv109I subpassages (Fig. 3*A* and *SI Appendix*, Fig. S7), resulting in two clearly different Bv109I-adapted strain at the third passage. Bv109I-adapted M-NO1 and M-NO2 were distinguishable by their different PrP$^{Sc}$ types (Fig. 3*A*), lesion profiles (Fig. 6*A*), and partially different PrP$^{Sc}$ deposition patterns (Fig. 6*B*), particularly in some white matter tracts, such as the internal and external capsules, the anterior and posterior commissures, and the corpus callosum (Fig. 6*C*).

Disease phenotypes were mostly preserved on third passages of E-CA1, M-CA1, and R-NO1 (Fig. 6 *A* and *B*), with R-NO1 showing a stronger involvement of auditory, motor, and especially, somatosensory cortices (Fig. 6*B*). Most importantly, the higher MW and amount of PrP$^{res}$ in voles infected with R-NO1 compared to E-CA1 and M-CA1 was also preserved on third passage (Fig. 6*D*). Thus, although the Norwegian reindeer and North American CWD isolates shared some pathological phenotypes in the original hosts and after transmission in Bv109I, we did not find evidence for the emergence of the fast Bv109I-adapted North American CWD strain from Norwegian reindeer isolates.

## Discussion

Acquiring knowledge of the characteristics of Norwegian prion strains is critical for proper management of these emergent forms of CWD. In order to trace back the possible origin of Norwegian CWD and to better understand its epidemiology, we characterized their strain properties and compared them with CWD strains from NA. An important finding in our study was that we did not find evidence of common strains between CWD cases derived from NA and Norway. This finding argues against a direct and recent epidemiological link between these emerging European CWD cases and the established CWD epidemic in NA, as it has been instead the case for CWD outbreaks in the Republic of Korea (5).

**Prion Strains and Cross-Species Transmission.** The current understanding of prion strains indicates that prion strains are composed of an ensemble of quasispecies conformations, and that a single PrP primary structure can adopt a defined portfolio of different PrP$^{Sc}$ conformations that encipher heritable, and in some cases mutable strain properties (27). Frequently, several PrP$^{Sc}$ conformations can be contained in a single prion isolate from natural hosts (27). Seminal studies suggested that rodent-adapted strains may stem from the separation of a single strain from a mixture (28). There is now evidence that some of the PrP$^{Sc}$ conformations present in natural prion isolates might be selectively propagated in different hosts or tissues (17, 20, 29, 30). These have been defined as "strain components" or "substrains."

The above considerations have important consequences for the interpretation of studies dealing with transmission of prion isolates from natural hosts to rodent models. Indeed, it is known that species barriers may drive the selective replication of prion strain components, leading to strain evolution or even mutation (27). This phenomenon depends mainly, but not exclusively (29, 31), on the different PrP primary structures of donor and recipient species, where the recipient species will selectively propagate only the conformations, if any, its own PrP can adopt (27). This implies that rodent-adapted strains may give an incomplete representation of the biological properties in the original prion isolate. Nevertheless, due to lack of a detailed molecular understanding of prion strains, bioassay in rodents remains the gold standard for prion strain typing. While the

resulting rodent-adapted strains cannot be considered to faithfully represent the whole biological properties of the original natural isolates, this approach can be reliably used to identify or exclude the biological identity of two or more prion sources (9–13).

The use of bank voles as a model system has certainly been pivotal for the present study. Indeed, bank voles and transgenic mice expressing bank vole PrP have been shown to faithfully propagate prion strains from various species (26, 31, 32), including prion strains that are difficult to transmit in other animal models (33, 34). We based our conclusions on a careful comparison of incubation times and pathological phenotypes induced by natural CWD isolates along three serial passages in the new host. Furthermore, we limited our interpretation to address the potential biological similarity of different CWD sources. Collectively, these considerations argue against the notion that the transmission barrier between cervids and vole might have played a major role in driving the main outcomes of our study.

**Different CWD Strains from NA and Norway.** Several studies in transgenic and gene targeted mice and conventional rodents suggest that some strain variation may be present among NA CWD isolates (35–38). A thorough investigation by transmission in transgenic and gene-targeted mice of a large collection of CWD isolates from NA, led to the conclusion that CWD isolates are composed of an ensemble of PrP$^{Sc}$ conformers, which are differentially selected and propagated by elk and deer PrP sequences (17, 19). Other studies with experimentally infected white-tailed deer of different PrP genotypes also support the notion that PrP sequence variation within cervid species could drive strain selection and evolution (39, 40). It is thus conceivable that the long-lasting outbreak of CWD in NA might result in variation of the ensemble of PrP$^{Sc}$ conformers in different cervid species and/or geographic locations, although all isolates might still share PrP$^{Sc}$ conformers or substrains.

We observed full overlap of transmission properties and disease phenotypes during three serial passages of US (24) and Canadian CWD isolates in Bv109I, implying the isolation of the same vole-adapted strain from all NA CWD isolates, regardless of cervid species and location in NA. Based on the above considerations, we conclude that Bv109I selectively propagated a strain component shared by all NA sources studied so far in this model. This suggests that these NA cases are epidemiologically related by the involvement of a prevalent CWD strain, which is driving the ongoing epidemic in the United States and Canada.

Importantly, we did not find evidence in any of the Norwegian isolates for the presence of the same CWD strain component isolated from NA CWD cases. All Bv109I-passaged Norwegian CWD isolates showed PrP$^{Sc}$ and neuropathological features clearly distinct from Bv109I-passaged NA CWD. Furthermore, the Norwegian CWD strains showed much slower replication kinetics in Bv109I than the NA-derived strain, with survival times approximately two to five times longer than the invariant ~35-d time to disease onset produced by NA-derived CWD (Table 1). It is thus conceivable that even low amounts of the NA CWD strain component, if present, would have outcompeted other strain components in the Norwegian CWD isolates. Importantly, as the characteristics of the Bv109I-adapted CWD strains isolated from elk, deer, and also moose from Canada were identical, we can conclude that CWD replication in moose does not lead per se to CWD strain mutation. Overall, these findings suggest that CWD in Norway is caused by prion strains that are not related to NA CWD.

**CWD Strain Variation in Norwegian Cervids.** In contrast to the uniform outcome observed with CWD isolates from different NA cervid species, three different strains were detected in only five
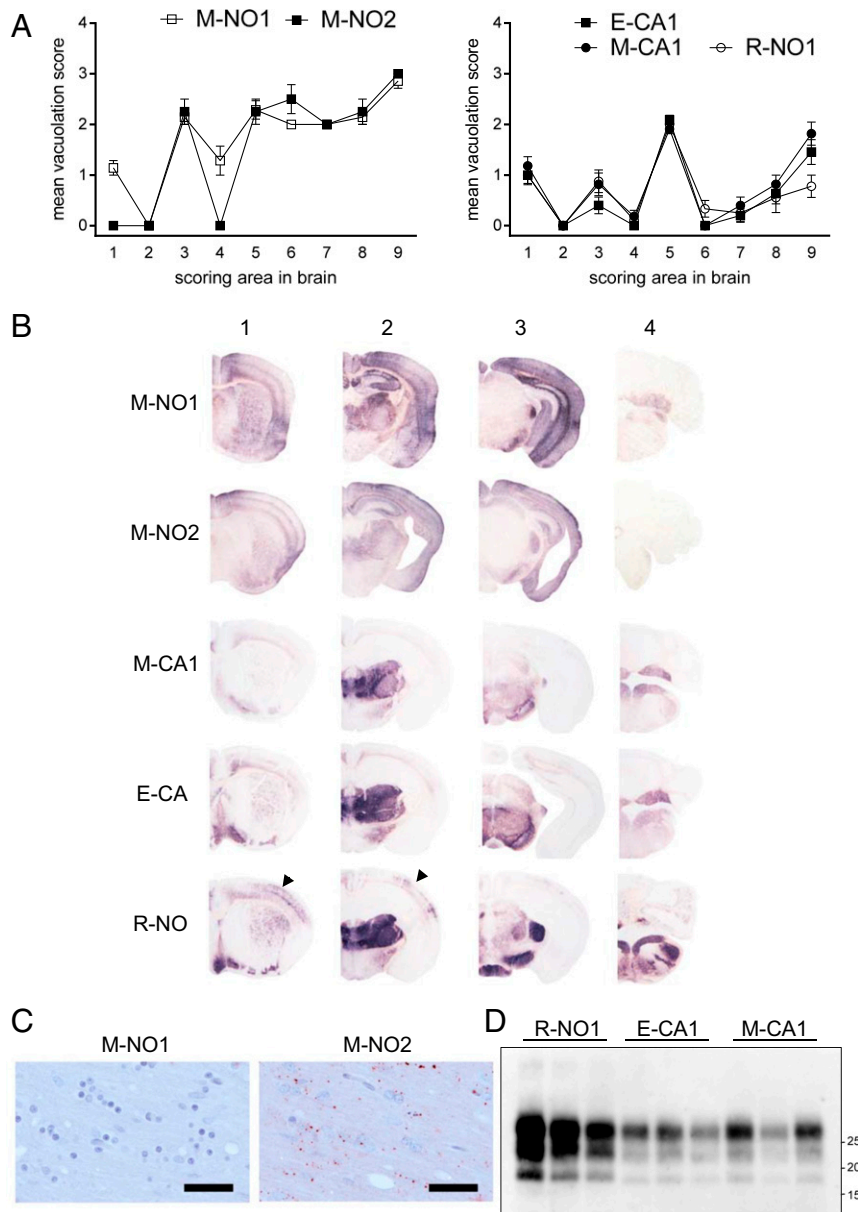
**Fig. 6.** Different neuropathological and PrP$^{Sc}$ phenotypes induced by Norwegian and Canadian CWD isolates after three passages in Bv109I. Comparison of neuropathological and molecular phenotypes for groups of Bv109I analyzed by different techniques shows four different phenotypes of disease in Bv109I-adapted CWD from Canadian isolates, M-NO1, M-NO2, and R-NO1, respectively. (*A*) Lesion profiles in Bv109I following the third passages of CWD isolates from Norwegian moose (M-NO1 and M-NO2, *Left*), Canadian CWD isolates and Norwegian reindeer (E-CA1, M-CA1, and R-NO1, *Right*). Data points represent the mean (SEM) of at least five voles per group. Brain-scoring areas: medulla (1), cerebellum (2), superior colliculus (3), hypothalamus (4), thalamus (5), hippocampus (6), septum (7), retrosplenial and adjacent motor cortex (8), and cingulate and adjacent motor cortex (9). (*B*) PET blot detection of protease-resistant PrP$^{Sc}$ in brain coronal sections representing telencephalon (1), diencephalon (2), midbrain (3), and hindbrain (4) from representative Bv109I after the third passages with the CWD isolates M-NO1, M-NO2, M-CA1, E-CA1, and R-NO1, as indicated. Note that, in agreement with the absence of spongiform degeneration in the medulla of Bv109I infected with M-NO2 but not with M-NO1 (see *A*), PrP$^{Sc}$ deposition in the hindbrain was low or absent in M-NO2. M-CA1 and E-CA1 showed a similar pattern of PrP$^{Sc}$ deposition, which was different from M-NO1 and M-NO2, in agreement with the different lesion profiles (see *A*). PrP$^{Sc}$ deposition in R-NO1 mostly overlapped with that in M-CA1 and E-CA1, but was characterized by the involvement of superficial cortical layers in the somatosensory cortex, which was absent in Bv109I infected with Canadian CWD isolates (arrowheads in coronal sections *A* and *B*). PrP$^{Sc}$ was detected with mAb SAF84. (*C*) Immunohistochemical detection of PrP$^{Sc}$ in the corpus callosum of Bv109I inoculated with the CWD isolates M-NO1 and M-NO2, showing PrP$^{Sc}$ deposition in Bv109I infected with M-NO2 but not in those with M-NO1. PrP was detected by mAb SAF84. (Scale bar: 50 μm.) (*D*) Western blot showing PK-treated PrP$^{Sc}$ from three Bv109I per group after second passages with R-NO1, E-CA1, and M-CA1, as indicated on the *Top* of the blot. PrP$^{Sc}$ was detected with mAb SAF84. The position of the MW markers is indicated on the *Right* of the blots (in kilodaltons).

cases sampled in Norway, one from reindeer and two from moose. These different outcomes might reflect different epidemiological situations in NA compared to Europe, possibly suggestive of distinct ecological situations. Whereas CWD in NA is mostly found in white-tailed deer, mule deer, and elk, natural CWD infections in moose are comparatively rare (6, 41, 42) and

to date have not been reported in wild reindeer/caribou. This contrasts with the emerging situation in Europe where, at the time of writing, CWD is detected in wild moose and reindeer, with the exception of one wild red deer (*Cervus elaphus*) (23, 43). Interestingly, CWD from Norwegian moose and reindeer showed completely different biological properties in our studies.

Moose CWD transmitted efficiently in Bv109I, while reindeer CWD was barely transmissible; accordingly, we derived distinct Bv109I-adapted CWD strains from reindeer and moose isolates. This argues against the hypothesis of an ongoing interspecies circulation of CWD in Norway, as also suggested by the figures emerging from the CWD surveillance in Norway (23).

Neuropathological characterization (21, 22) and early PrP$^{Sc}$ deposition in lymphoid tissues (23) in Norwegian reindeer concurred in suggesting similarities with CWD in NA. Thus, we were surprised that reindeer isolates were so poorly transmissible in Bv109I, despite the sensitivity of this animal model to NA CWD (24). Serial passages of the only Bv109I positive after reindeer inoculations did not lead to the isolation of the NA CWD strain, but to a Bv109I-adapted CWD strain with noticeably slower disease kinetics and different PrP$^{Sc}$ conformation, as determined by PrP$^{res}$ typing. However, Bv109I-adapted reindeer CWD was characterized by a brain distribution of spongiosis and PrP$^{Sc}$ deposition partially overlapping with NA isolates, thus paralleling the observations in the original hosts (21, 22). We conclude that reindeer and NA CWD are characterized by two different CWD strains, possibly having similar neurotoxic pathways.

While the epidemiology of CWD in reindeer from the Nordfjella region suggests the contagious nature of the disease (44, 45), disease etiology in other species in Norway is less well understood. So far, CWD has been detected in one red deer and seven moose in Norway, and in four other moose in the Nordic European Union countries, one in Finland and three in Sweden (23). These cases were all characterized by advanced age (between 10 and 20 y), by atypical neuropathological and PrP$^{Sc}$ features, and by the absence of detectable PrP$^{Sc}$ in lymphoid tissues (23). Our results confirm that these atypical disease features were indeed the manifestation of CWD strain(s) that are different from NA and Norwegian reindeer CWD strains.

In an ongoing effort to characterize all cases detected in Europe, we detected some biochemical differences among the first three cases in moose, with M-NO1 being slightly different from M-NO2 and M-NO3 (22). Indeed, in the present study, we isolated two different Bv109I-adapted strains from these CWD cases. Besides having different incubation times and partially different PrP$^{Sc}$ types, Bv109I-adapted moose CWD strains also shared peculiar features, i.e., the strong neurodegeneration in cortex and hippocampus accompanied by intraneuronal PrP$^{Sc}$ deposits and the presence of an unusual 12- to 13-kDa C-terminal PrP$^{res}$ fragment. These pathological features were both reminiscent of the disease in the original host (22) and distinct from the CWD strains detected in NA cervids and reindeer in Norway. Another interesting feature was the slow adaptation of M-NO2, which might suggest an ongoing competition between different strain components being selected during adaptation in Bv109I. The characterization of further moose CWD isolates will help to better define the CWD strain variation in Nordic moose.

The detection of two moose CWD cases (M-NO1 and M-NO2) within a time span of 2 wk and a distance of 20 to 30 km in the Selbu region of Norway suggests an epidemiological relationship between them. However, this hypothesis is difficult to reconcile with our isolation of two different CWD strains from these two animals, and the lack of detectable lymphoid involvement argues against a contagious CWD strain in CWD-affected Nordic moose.

Some animal prion diseases, including atypical H- and L-BSE strains in cattle and Nor98/atypical scrapie in sheep and goats, occur sporadically and are considered to be spontaneous in origin. In line with the advanced age of the affected moose and with the absence of detectable lymphoid involvement (22), it has been hypothesized that CWD in Norwegian moose could represent one such sporadic animal prion diseases (23). The isolation of two different CWD strains in moose in Norway is compatible with such a scenario, similarly to what happens with the multiple sporadic CJD strains in humans (46) and with the two atypical BSE strains in cattle (3). However, the possibility that the disease in Norwegian moose represents a spontaneous prion disease would not explain the apparent spatial clusters of cases emerging from surveillance activities in Norway and Sweden (23), nor the lack of evidence in NA for CWD cases similar to those detected in Europe, even if both could be explained by biased surveillance methods. The continuing surveillance in Europe and NA in the coming years will hopefully ascertain the actual distribution of the disease in susceptible species of European cervids and the possible presence of atypical strains in NA moose.

## Conclusions

Our finding that CWD in European cervids is caused by prion strains with properties different from the prevalent CWD strain that currently sustains the NA epidemic has important implications for understanding the origin and nature of CWD in Europe. The variety of strains observed in Norwegian cervid species raises questions about the ecology of the disease compared to NA and has implications for the proper targeting of surveillance efforts and control strategies in Europe. Most importantly, all of the available knowledge about diagnostics, pathogenesis, transmissibility, species range, and zoonotic potential of CWD derive from the study of NA CWD. Since the CWD strains in Europe are different from NA CWD, the present knowledge is not easily transferrable to the European situation and a reevaluation of the transmissibility and the zoonotic potential of the new CWD strains here identified is needed.

## Materials and Methods

**Animals.** Bank voles carrying isoleucine at the polymorphic *PRNP* codon 109 (Bv109I) (47) were obtained from the breeding colony of Istituto Superiore di Sanità (ISS). The experimental protocol was approved and supervised by the Service for Biotechnology and Animal Welfare of the Istituto Superiore di Sanità and authorized by the Italian Ministry of Health (decree number 1119/2015-PR). All procedures were carried out in accordance with European Council directives 86/609 and 2010/63, as well as in compliance with the Italian Legislative Decree 26/2014.

**CWD Isolates.** Most of the CWD isolates used to produce the inocula for the present study have been previously characterized for their PrP$^{Sc}$ biochemical properties and are described in detail there (22). The *PRNP* genotype of these CWD isolates has been determined in previous studies (22, 48). The species, geographical origin, age, *PRNP* genotype, and ID number of the CWD cases are reported in *SI Appendix*, Table S1.

**Bioassay.** For primary passages, 10% (wt/vol) brain homogenates in PBS were prepared from brain tissues from the CWD cases reported in *SI Appendix*, Table S1. Similar preparations from half bank vole prion-positive brains were used for subpassages in bank voles. Eight-week-old Bv109I were inoculated with 20 μL of brain homogenate into the left cerebral hemisphere, under ketamine anesthesia (ketamine, 0.1 μg/g). The animals were examined twice a week until the appearance of neurological signs, and daily thereafter. Neurological signs ranged from mild behavioral alterations and the disappearance of the typical behavior of hiding under the sawdust lining the cage at disease onset, to dorsal kyphosis, severe ataxia, and head bobbing in full-blown disease. Diseased animals were culled with carbon dioxide at the terminal stage of the disease, but before the severity of neurological impairment compromised their welfare, in particular their ability to drink and feed adequately. At postmortem, brains from inoculated mice were removed and divided sagittally. Half the brain was frozen, and half was fixed in formol-saline for histological analyses. The attack rate was calculated as the number of animals scoring positive by WB and pathological diagnosis at postmortem/number inoculated. For primary transmissions, animals found dead or culled for intercurrent disease before 200 dpi and scoring negative at postmortem were excluded from analyses. The survival time for animals

scoring positive at postmortem was calculated as the time from inoculation to culling or death.

**Antibodies.** Purified PrP-specific mAbs were as follows: 12B2 (WBVR), Sha31 and SAF84 (SpiBio), and L42 (R-Biopharm). The mapped amino acid sequences (reindeer or moose PrP numbering) of these mAbs are as follows: 93WGQGG97 for 12B2; 148YEDRYYRE155 for Sha31; 167YRPVDQY172 for SAF84; and 148YEDRYY153 for L42. Based on their respective epitopes, these antibodies can be grouped into three categories: 1) 12B2 recognizes an epitope at the N terminus of PrP$^{res}$, which can be differentially cleaved by PK in different Bv109I-adapted prion strains (49) and is thus useful for discrimination. 2) Sha31 and L42 recognize epitopes in the core of PrP$^{res}$; and 3) SAF84 recognizes a C-terminal epitope and is able to detect not only the main C-terminal PrP$^{res}$ fragment, but also a shorter C-terminal fragment of around 10 to 14 kDa and its two glycosylated forms not detected by mAbs in the previous groups. This antibody helps to characterize the PrP$^{Sc}$ types in Bv109I-adapted strains (49) and in moose with CWD from Norway (22).

**Western Blot Analysis of PrP$^{Sc}$.** The overall biochemical approach to PrP$^{res}$ typing and epitope mapping in bank voles was as previously described (49) with minor modifications. PK was added at a final concentration of 100 μg/mL, and then the samples were incubated for 1 h at 55 °C with gentle shaking. For the analysis of PrP$^{res}$ in the inocula from cervids, PK was 50 μg/mL and the samples were incubated for 1 h at 37 °C. Deglycosylation was performed by adding 18 μL of 0.2 mmol/L sodium phosphate buffer (pH 7.4) containing 0.8% Nonidet P-40 (Roche) and 2 μL (80 U/mL) di N-Glycosidase F (Roche) to 5 μL of PK-digested and denatured samples for 3 h at 37 °C. After electrophoresis on 12% bis-Tris polyacrylamide gels (Invitrogen) and WB on polyvinylidene fluoride membranes using the Trans-Blot Turbo Transfer System (Bio-Rad), the blots were processed with anti-PrP mAbs by using the SNAP i.d. 2.0 system (Millipore). PrP$^{res}$ was detected with mAbs SAF84, Sha31, and 12B2 in Bv109I and with mAbs SAF84 and L42 in cervid isolates.

PrP was visualized by enhanced chemiluminescent substrate and the ChemiDoc imaging system (Bio-Rad). The chemiluminescent signal was quantified by Image Lab software (Bio-Rad). The Sha31/12B2 antibody ratio was used in order to discriminate PrP$^{res}$ types with different N-terminal PK-cleavage sites. The Sha31/12B2 absolute ratio was determined by calculating the chemiluminescence signal of PrP$^{res}$ separately with Sha31 and 12B2 monoclonal antibodies. To obtain the relative Sha31/12B2 ratio, we calculated the absolute ratio of Sha31/12B2 volumes for each sample and for Bv109I-adapted scrapie used as reference and then divided the absolute ratio of each sample by the absolute ratio of the scrapie control.

**Histopathology, Immunohistochemistry, Lesion Profile, and PET Blot.** Histology and immunohistochemistry analyses were performed on formalin-fixed tissues as previously described (26). Briefly, coronal brain sections were obtained from four antero-posterior levels including the following: 1) telencephalon at midlevel of caudate nucleus, 2) diencephalon at midlevel of thalamus, 3) midbrain, and 4) hindbrain at midlevel of medulla and cerebellum. Microscopic examinations were carried out on sections stained with hematoxylin and eosin or probed with mAb SAF84. For the construction of lesion profiles, vacuolar changes were scored in nine gray-matter areas of the brain on hematoxylin and eosin-stained sections (25). Vacuolation scores are derived from at least five individual voles per group and are reported as means ± SEM. PET blot was carried out on the same four levels coronal sections, as previously described (26), using mAb SAF84.

1. J. W. Ironside, D. L. Ritchie, M. W. Head, Prion diseases. *Handb. Clin. Neurol.* **145**, 393–403 (2017).
2. R. Knight, Infectious and sporadic prion diseases. *Prog. Mol. Biol. Transl. Sci.* **150**, 293–318 (2017).
3. F. Houston, O. Andréoletti, Animal prion diseases: The risks to human health. *Brain Pathol.* **29**, 248–262 (2019).
4. N. A. Rivera, A. L. Brandt, J. E. Novakofski, N. E. Mateus-Pinilla, Chronic wasting disease in cervids: Prevalence, impact and management strategies. *Vet. Med. (Auckl.)* **10**, 123–139 (2019).
5. T. Y. Kim et al., Additional cases of chronic wasting disease in imported deer in Korea. *J. Vet. Med. Sci.* **67**, 753–759 (2005).
6. J. A. Moreno, G. C. Telling, Molecular mechanisms of chronic wasting disease prion propagation. *Cold Spring Harb. Perspect. Med.* **8**, a024448 (2018).
7. R. A. Bessen, R. F. Marsh, Distinct PrP properties suggest the molecular basis of strain variation in transmissible mink encephalopathy. *J. Virol.* **68**, 7859–7868 (1994).
8. G. C. Telling et al., Evidence for the conformation of the pathologic isoform of the prion protein enciphering and propagating prion diversity. *Science* **274**, 2079–2082 (1996).
9. A. Kobayashi, M. Asano, S. Mohri, T. Kitamoto, A traceback phenomenon can reveal the origin of prion infection. *Neuropathology* **29**, 619–624 (2009).
10. A. Kobayashi et al., Transmission properties of atypical Creutzfeldt-Jakob disease: A clue to disease etiology? *J. Virol.* **89**, 3939–3946 (2015).
11. M. E. Bruce et al., Transmissions to mice indicate that "new variant" CJD is caused by the BSE agent. *Nature* **389**, 498–501 (1997).
12. A. F. Hill et al., The same prion strain causes vCJD and BSE. *Nature* **389**, 448–450, 526 (1997).
13. M. Eloit et al., BSE agent signatures in a goat. *Vet. Rec.* **156**, 523–524 (2005).
14. H. Cassard et al., Evidence for zoonotic potential of ovine scrapie prions. *Nat. Commun.* **5**, 5821 (2014).
15. A. Huor et al., The emergence of classical BSE from atypical/Nor98 scrapie. *Proc. Natl. Acad. Sci. U.S.A.* **116**, 26853–26862 (2019).
16. M. E. Bruce et al., Strain characterization of natural sheep scrapie and comparison with BSE. *J. Gen. Virol.* **83**, 695–704 (2002).
17. R. C. Angers et al., Prion strain mutation determined by prion protein conformational compatibility and primary structure. *Science* **328**, 1154–1158 (2010).
18. A. Herbst, C. D. Velásquez, E. Triscott, J. M. Aiken, D. McKenzie, Chronic wasting disease prion strain emergence and host range expansion. *Emerg. Infect. Dis.* **23**, 1598–1600 (2017).
19. J. Bian et al., Primary structural differences at residue 226 of deer and elk PrP dictate selection of distinct CWD prion strains in gene-targeted mice. *Proc. Natl. Acad. Sci. U.S.A.* **116**, 12478–12487 (2019).
20. R. Nonno et al., Characterization of goat prions demonstrates geographical variation of scrapie strains in Europe and reveals the composite nature of prion strains. *Sci. Rep.* **10**, 19 (2020).
21. S. L. Benestad, G. Mitchell, M. Simmons, B. Ytrehus, T. Vikøren, First case of chronic wasting disease in Europe in a Norwegian free-ranging reindeer. *Vet. Res. (Faisalabad)* **47**, 88 (2016).
22. L. Pirisinu et al., Novel type of chronic wasting disease detected in moose (*Alces alces*), Norway. *Emerg. Infect. Dis.* **24**, 2210–2218 (2018).
23. EFSA Panel on Biological Hazards; K. Koutsoumania et al., Scientific opinion on the update on chronic wasting disease (CWD) III. *EFSA J.* **17**, 5863 (2019).
24. M. A. Di Bari et al., Chronic wasting disease in bank voles: Characterisation of the shortest incubation time model for prion diseases. *PLoS Pathog.* **9**, e1003219 (2013).
25. H. Fraser, A. G. Dickinson, The sequential development of the brain lesion of scrapie in three strains of mice. *J. Comp. Pathol.* **78**, 301–311 (1968).
26. R. Nonno et al., Efficient transmission and characterization of Creutzfeldt-Jakob disease strains in bank voles. *PLoS Pathog.* **2**, e12 (2006).
27. J. Collinge, A. R. Clarke, A general model of prion strains and their pathogenicity. *Science* **318**, 930–936 (2007).
28. R. H. Kimberlin, C. A. Walker, Evidence that the transmission of one source of scrapie agent to hamsters involves separation of agent strains from a mixture. *J. Gen. Virol.* **39**, 487–496 (1978).
29. A. Le Dur et al., Divergent prion strain evolution driven by PrP$^C$ expression level in transgenic mice. *Nat. Commun.* **8**, 14170 (2017).
30. V. Béringue et al., Host prion protein expression levels impact prion tropism for the spleen. *PLoS Pathog.* **16**, e1008283 (2020).
31. J. C. Espinosa et al., PrP$^C$ governs susceptibility to prion strains in bank vole, while other host factors modulate strain features. *J. Virol.* **90**, 10660–10669 (2016).
32. J. C. Watts et al., Evidence that bank vole PrP is a universal acceptor for prions. *PLoS Pathog.* **10**, e1003990 (2014).
33. L. Pirisinu et al., Gerstmann-Sträussler-Scheinker disease subtypes efficiently transmit in bank voles as genuine prion diseases. *Sci. Rep.* **6**, 20443 (2016).
34. R. Nonno et al., Variable protease-sensitive prionopathy transmission to bank voles. *Emerg. Infect. Dis.* **25**, 73–81 (2019).
35. S. R. Browning et al., Transmission of prions from mule deer and elk with chronic wasting disease to transgenic mice expressing cervid PrP. *J. Virol.* **78**, 13345–13350 (2004).
36. G. LaFauci et al., Passage of chronic wasting disease prion into transgenic mice expressing Rocky Mountain elk (*Cervus elaphus nelsoni*) PrP$^C$. *J. Gen. Virol.* **87**, 3773–3780 (2006).
37. G. Tamgüney et al., Transmission of elk and deer prions to transgenic mice. *J. Virol.* **80**, 9104–9114 (2006).

38. G. J. Raymond *et al.*, Transmission and adaptation of chronic wasting disease to hamsters and transgenic mice: Evidence for strains. *J. Virol.* **81**, 4305–4314 (2007).

39. C. Duque Velásquez *et al.*, Deer prion proteins modulate the emergence and adaptation of chronic wasting disease strains. *J. Virol.* **89**, 12362–12373 (2015).

40. J. Moore *et al.*, Novel strain of the chronic wasting disease agent isolated from experimentally inoculated elk with LL132 prion protein. *Sci. Rep.* **10**, 3148 (2020).

41. L. A. Baeten, B. E. Powers, J. E. Jewell, T. R. Spraker, M. W. Miller, A natural case of chronic wasting disease in a free-ranging moose (*Alces alces shirasi*). *J. Wildl. Dis.* **43**, 309–314 (2007).

42. N. J. Haley, E. A. Hoover, Chronic wasting disease of cervids: Current knowledge and future perspectives. *Annu. Rev. Anim. Biosci.* **3**, 305–325 (2015).

43. T. Vikøren *et al.*, First detection of chronic wasting disease in a wild red deer (*Cervus elaphus*) in Europe. *J. Wildl. Dis.* **55**, 970–972 (2019).

44. A. Mysterud, C. M. Rolandsen, A reindeer cull to prevent chronic wasting disease in Europe. *Nat. Ecol. Evol.* **2**, 1343–1345 (2018).

45. H. Viljugrein *et al.*, A method that accounts for differential detectability in mixed samples of long-term infections with applications to the case of chronic wasting disease in cervids. *Methods Ecol. Evol.* **10**, 134–145 (2019).

46. M. Rossi, S. Baiardi, P. Parchi, Understanding prion strains: Evidence from studies of the disease forms affecting humans. *Viruses* **11**, 309 (2019).

47. C. Cartoni *et al.*, Identification of the pathological prion protein allotypes in scrapie-infected heterozygous bank voles (*Clethrionomys glareolus*) by high-performance liquid chromatography-mass spectrometry. *J. Chromatogr. A* **1081**, 122–126 (2005).

48. M. E. Güere *et al.*, Chronic wasting disease associated with prion protein gene (*PRNP*) variation in Norwegian wild reindeer (*Rangifer tarandus*). *Prion* **14**, 1–10 (2020).

49. L. Pirisinu *et al.*, Biochemical characterization of prion strains in bank voles. *Pathogens* **2**, 446–456 (2013).